

Properties of the electron-hole plasma in II-VI compounds as a function of temperature

H.-E. Swoboda, M. Sence,* F. A. Majumder, M. Rinker, J.-Y. Bigot,*
J. B. Grun,* and C. Klingshirn

Fachbereich Physik, Universität Kaiserslautern, Erwin-Schrödinger-Strasse, D-6750 Kaiserslautern, West Germany

(Received 3 January 1989)

We present time-integrated and time-resolved luminescence and gain investigations in CdS and CdSe under low and high excitation for temperatures between liquid-helium and room temperature. We observe an increase of the density and the lifetime of the carriers and a decrease of their drift length with increasing temperature. The results are compared with measurements of other II-VI compounds. The findings are discussed in the frame of the many-particle theory for an electron-hole plasma and compared to some universal approaches to the band-gap renormalization presented in other works.

I. INTRODUCTION

During the last decade, the investigation of nonlinear optical systems has been found to be of great interest, partly because of potential applications concerning optical data processing. One particular phenomenon, which is connected with huge optical nonlinearities is the transition to an electron-hole plasma under intense laser excitation. The characteristics of this plasma, e.g., the density, the lateral and longitudinal drift length, and the properties at various temperatures have been extensively studied in CdS (see, e.g., Refs. 1 and 2 and references given therein). The aim of this paper is to present new results from time-integrated and time-resolved measurements for CdSe and to compare them with those known for CdS. Moreover, new results of time-resolved gain spectroscopy in CdS are reported. We carried out luminescence and gain spectroscopy in the range between liquid-helium and room temperature under low and high excitation. In these experiments we observed the transition from a degenerate electron-hole plasma, where the filling of the bands is described by quasi-Fermi functions for electrons and holes, respectively, to the nondegenerate situation. This transition occurs around 150 K. The behavior of certain parameters is discussed which determine this transition, e.g., the lifetime and the drift length of the plasma as well as the temperature dependence of the stimulated emission. In connection with higher temperatures, the so-called Urbach-Martienssen tail in the absorption will be treated. In general, the results found for CdSe are comparable to those for CdS.

Furthermore, recent and older approaches to universal description of the behavior of the band-gap shrinkage due to many-particle effects in highly excited systems will be discussed and related to our experimental results. In this connection a comparison with measurements on various II-VI compounds such as CdS, CdSe, CdTe, and ZnO reveals the validity of these universal expressions only to a certain extent. Finally, the differences will be outlined between these pure crystals and the mixed crystal $\text{CdS}_{1-x}\text{Se}_x$, where localization effects can be observed.

This paper is organized in the following way. Section

II contains the description of the time-integrated and time-resolved luminescence and two-beam methods together with some remarks on the crystals under investigation, since there are some discrepancies to earlier measurements. In Sec. III we report the results of the luminescence experiments in CdSe under low and high excitation. In Sec. IV we describe the results of the time-integrated and time-resolved gain spectroscopy as a function of the temperature in CdS and CdSe, whereas in Sec. V the drift length of the electron-hole plasma at increased temperature is discussed. Finally, Secs. VI and VII are dedicated to the comparison of the results with some universal laws and with the optical behavior known from mixed crystals, respectively.

II. EXPERIMENTAL SETUP AND CRYSTALS

The experimental techniques used were common pump-and-probe-transmission and reflection spectroscopies. For the time-resolved luminescence measurements we worked with an excimer XeCl laser (EMG 101-Lambda Physic) as the central pump source. The other experiments were done with a nitrogen laser (UV 400-Moletron). In both setups these lasers were used to pump two dye lasers. The crystal was excited by an intense tunable narrow-band dye laser, mounted in a Hänsch configuration, with a light field polarized $\mathbf{k} \perp \mathbf{c}$, $\mathbf{E} \parallel \mathbf{c}$, where \mathbf{k} is the wave vector of the light field, \mathbf{E} its electric field, and \mathbf{c} the crystallographic axis. The transmission or reflection of a spectrally broad low-intensity probe was recorded. The samples are high-quality platelets with a thickness of 2–20 μm grown by a vapor phase transport method. We found some discrepancy concerning the energetic position of the exciton in CdSe. Depending on the sample, the exciton resonances were blue shifted by 5–8 meV compared to literature data of $A\Gamma_5^T = 1.825$ eV.³ This phenomenon appeared both in samples grown in the crystal laboratories in Strasbourg and in Karlsruhe, and was measured independently in the laboratories of Strasbourg and of Kaiserslautern. By means of atomic absorption measurements, we found that the concentration of Cu, Ni, Zn, Al,

Te, Mg, and K in our crystals was lower than about a tenth of a ppm. We also checked the concentration of S by neutron activation. It was found to be below the detection limit of $\leq 1\%$. So the reason for the blue shift is presently not clear.

The dyes used were DCM solved in DMSO in the experiments concerning CdSe, and Coumarin 102 and Coumarin 307 for CdS, respectively. The luminescence resulting from the excitation was subtracted from the recorded probe beam spectra. The spot diameter of the exciting beam on the crystal ($d=60\ \mu\text{m}$) was twice as large as the one of the probe beam in order to ensure that the polychromatic laser probes a homogeneously excited crystal. The spatial and temporal coincidence of the two beams on the crystal was checked carefully. For the determination of the longitudinal expansion of the electron-hole plasma into the crystal, we measured the disappearance of the excitonic reflection structure on the unexcited surface of the crystal platelet. By using the thickness of the crystal as a parameter, we determined the drift length of the plasma l_d .² Independently, l_d could be determined by evaluating the behavior of the integrated optical amplification of the probe beam as a function of the crystal thickness.²

The length of the laser pulses was 5 and 3 ns full width at half maximum (FWHM) for the pump beam and the probe beam, respectively. In the time-resolved investigations, therefore, we probed continuously the temporal evolution of the optical properties of the crystal during the excitation pulse in contrast to more-common experiments, where the recombination after a δ -pulse excitation is monitored. Under these conditions we observed a sequence of quasistationary states, following the intensity of the exciting laser with a specific delay, depending on the temperature. We recorded the transmission and reflection spectra after dispersion by a 1-m spectrometer with an optical multichannel analyzer (OMA II and WP IV, respectively). In the time-resolved measurements we worked with a streak camera (ARP and Hadland, respectively) in front of the recording system. We used a temporal resolution of 100 ps in the luminescence experiments and 200 ps in the two-beam measurements, respectively.

III. LUMINESCENCE

A. Time-integrated luminescence

Since the results for CdS have been presented elsewhere (see, e.g., Ref. 4), we show here only the spectra for CdSe. With increasing excitation intensity we observe three characteristic features in the luminescence spectra. This is shown in Fig. 1. At low intensities [$I_{\text{exc}}=20\ \text{kW cm}^{-2}$, Fig. 1(a)], the spectrum is governed by a peak at 1.827 eV, which corresponds to the spectral position of the bound exciton I_2 , again blue shifted by 5 meV [$I_2=1.822\ \text{eV}$ (Ref. 3)]. 2 meV below the bound exciton, another feature can be distinguished, which can be identified with the M band. The M band is situated, as in other wurtzite II-VI materials, on the low-energy side of a bound-exciton complex, which makes a unique assignment difficult.⁴ The interpretation in terms of biexciton

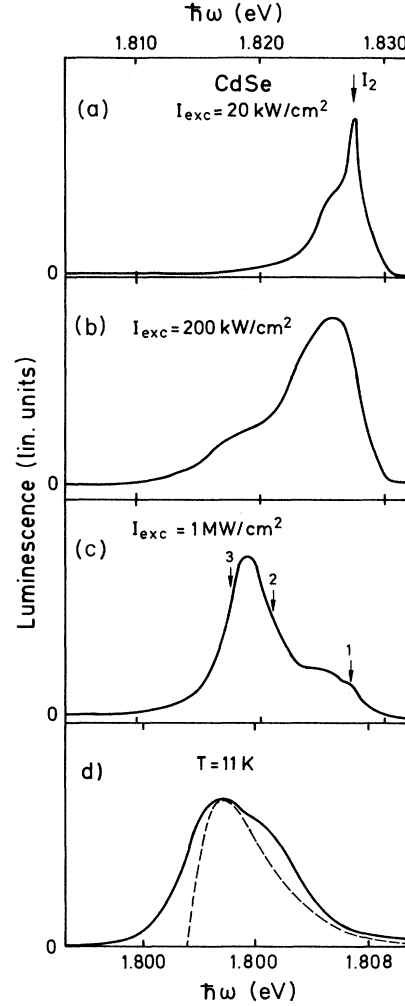


FIG. 1. Time-integrated luminescence spectra of thin CdSe platelets at $T_1=2\ \text{K}$ for increasing excitation intensity $I_{\text{exc}}=(\text{a})\ 20\ \text{kW cm}^{-2}$, (b) $200\ \text{kW cm}^{-2}$, and (c) $1\ \text{MW cm}^{-2}$. “1,” “2,” and “3” in (c) correspond to the energetic positions, where the results of Fig. 2 are obtained. Part (d) shows the luminescence spectrum of a thick crystal for $I_{\text{exc}}=1\ \text{MW cm}^{-2}$. The excitation energy was 1.846 eV in all cases.

decay would result in a biexciton binding energy of 5 meV. This value is in agreement with data from recent four-wave mixing measurements⁵ and from literature.³

The peak broadens and increases with increasing excitation intensity, and a new broad band appears at around 1.820 eV [$I_{\text{exc}}=200\ \text{kW cm}^{-2}$, see Fig. 1(b)]. We identified this broad band as the spontaneous luminescence of the electron-hole plasma, which is created at higher intensities. The shift to lower energies reflects the shrinkage of the band edge, due to many-particle effects. At even higher intensities the spectrum is governed by stimulated emission appearing at the low-energy flank of the plasma luminescence, see Fig. 1(c) ($I_{\text{exc}}=1\ \text{MW cm}^{-2}$). The M band mentioned above can still be identified in Fig. 1(c) as a structure at the high-energy side. It survives at these high excitation intensities due to

spatial and temporal density inhomogeneities.

These findings are representative for crystals with a small thickness $d \leq 10 \mu\text{m}$. In Fig. 1(d) we present a spectrum of a thicker crystal ($d = 20 \mu\text{m}$). Here we observe only one main luminescence band at high intensities. Its spectral position is 27 meV below the position of the free exciton as determined from the reflection spectra of this sample. This difference corresponds to the energy of a LO phonon in CdSe. The probability for the recombination of an exciton under emission of a LO phonon is higher in these thick crystals,⁶ and the luminescence of the electron-hole plasma is drastically reduced. Moreover, the density of the electron-hole plasma decreases with increasing crystal thickness due to the drift of the plasma out of the excited region. This is valid as long as the drift length (in CdSe, 12 μm) exceeds the thickness of the crystal. In addition, other experiments in CdS and ZnO have shown that in thicker crystals those processes are more probable, which have a small gain and small threshold intensities.^{4,6}

We have fitted the shape of the LO-phonon emission band with a simple model assuming that it can be described by the formula given by Gross *et al.* and Permogorov:⁷

$$J(\epsilon) = \sqrt{\epsilon} \exp\left[-\frac{\epsilon}{kT}\right] W(\epsilon),$$

where $W(\epsilon)$ is the probability of the first-order LO-phonon-assisted annihilation for the exciton with the kinetic energy ϵ . In their experimental studies of exciton luminescence in CdSe, Abramov *et al.*⁸ have shown that the first LO-phonon replica can be described with great accuracy by

$$J(\epsilon) \simeq \epsilon^{1.5} \exp\left[-\frac{\epsilon}{kT}\right]. \quad (1)$$

From a fit with this formula we get the dashed curve shown in Fig. 1(d), which agrees well with the experimental findings and yields a temperature of the exciton gas of 11 K. The small deviations at the low-energy edge are due to polariton effects not considered in Eq. (1). Data for ZnO are given in, e.g., Ref. 9.

B. Time-resolved luminescence

Figure 2 shows the temporal behavior of the intensity of the luminescence of a thin sample at different energetic positions within the main bands indicated in Fig. 1(c), during high excitation with ns pulses. The curves in Figs. 2(a)-2(c) are taken at the energies denoted in Fig. 1(c) as "1," "2," and "3," lying at the high-energy flank of the M band [Fig. 2(a)], at the high-energy flank of the plasma luminescence [Fig. 2(b)], and at its low-energy flank within the stimulated emission [Fig. 2(c)]. The modes observable in all three curves partly reflect the temporal shape of the exciting laser. At the beginning of the excitation pulse we obtain luminescence from the M band seen in Fig. 2(a) ($\hbar\omega = 1.827 \text{ eV}$) as a sharp peak. When the excitation intensity I_{exc} is high enough for the forma-

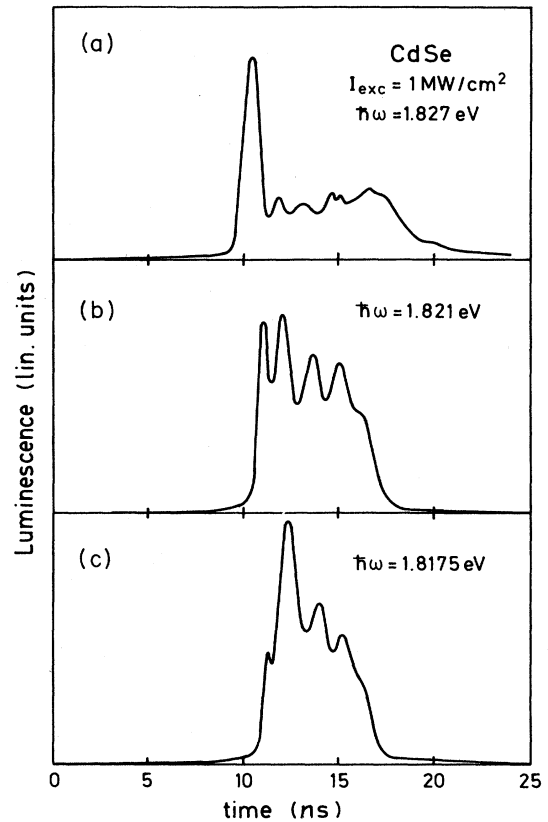


FIG. 2. Time-resolved luminescence of CdSe, taken at the energy of (a) the M band, (b) the high-energy sides, and (c) the low-energy sides of the plasma luminescence band, respectively [see Fig. 1(c)]. The conditions of excitation are the same as in Fig. 1(c).

tion of an electron-hole plasma, the plasma luminescence sets in [Fig. 2(b), $\hbar\omega = 1.82 \text{ eV}$] and reduces strongly the contribution from the M band. At highest intensities even stimulated luminescence occurs [Fig. 2(c), $\hbar\omega = 1.8175 \text{ eV}$]. At the end of the excitation pulse the contribution of the M band partly recovers [Fig. 2(a)] before the luminescence decays within 1 ns after the end of the excitation pulse. The stimulated emission, in turn, already decays with decreasing $I_{\text{exc}}(t)$ before the end of the excitation pulse and thus has a shorter temporal halfwidth, as expected.

IV. THE GAIN SPECTRA

A. Time-integrated measurements

In CdSe and CdS as in most of the direct-gap semiconductors, we can observe the formation of an electron-hole plasma under high laser excitation best in gain spectroscopy (see, for example, Refs. 1, 2, and 4). This phenomenon is connected with the changes of the optical properties observed, e.g., in the transmission spectra, shown in Fig. 3 for CdSe for increasing excitation intensities at low temperature. Starting at low intensities (last curve) one can clearly observe the exciton resonances of

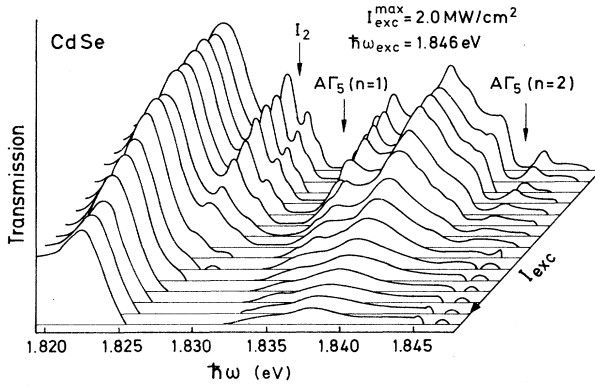


FIG. 3. Transmission spectra of CdSe at low temperatures for increasing excitation intensities, starting with the curve at the back. The maximum value of I_{exc} is 2 MW cm^{-2} , $\hbar\omega_{\text{exc}} = 1.846 \text{ eV}$. The resonances of the $A\Gamma_5$ and I_2 excitons are shown.

the I_2 exciton (1.828 eV), the $A\Gamma_5(n=1)$ (1.831 eV), and the $A\Gamma_5(n=2)$ exciton (1.843 eV), respectively, at the high-energy side of the absorption edge. All resonances are blue shifted by an amount of 6 meV (see above). Between the resonances and below the absorption edge, the Fabry-Perot modes of the crystal can be observed.

With increasing excitation intensity, we find a continuous red shift of the absorption edge due to the shrinkage of the band gap, and the broadening and decrease of the exciton resonances. The $n=2$ resonance disappears at lower intensities than the $n=1$ resonance, due to the smaller oscillator strength and larger Bohr radius. The band-gap renormalization leads to the decrease of the mode structures mentioned above. In addition, the modes are also blue shifted, due to the changes of the refractive index. The band filling which leads to optical amplification (gain) on the low-energy side cannot be seen in Fig. 3, due to the spectral resolution. Typical spectra for the optical amplification in CdS and CdSe are shown, e.g., in Ref. 2.

We can fit the measured gain spectra deduced from the transmission and shown in Fig. 4 (solid lines) using the many-body theory developed, e.g., in Ref. 10. The gain spectra are defined as the logarithm of the ratio of the transmission of the probe beam through the crystal under excitation to the transmission without excitation. The spectral region for gain reaches from the reduced band gap at the low-energy side up to the chemical potential of the electron-hole plasma at the high-energy side. We find values for the plasma density n_p in CdSe at a temperature of 15 K of around $3 \times 10^{17} \text{ cm}^{-3}$ for excitation intensities of around 1 MW cm^{-2} [Fig. 4(a), dashed line]. Higher values of n_p as presented in Ref. 2 have been achieved with higher excitation intensities. This is again a proof that the electron-hole plasma (EHP) is not in a liquidlike state (see also Ref. 1).

The temperature given above reflects the temperature of the plasma T_p , which differs slightly from the lattice temperature T_l ($T_l = 5 \text{ K}$). In CdS and CdSe the

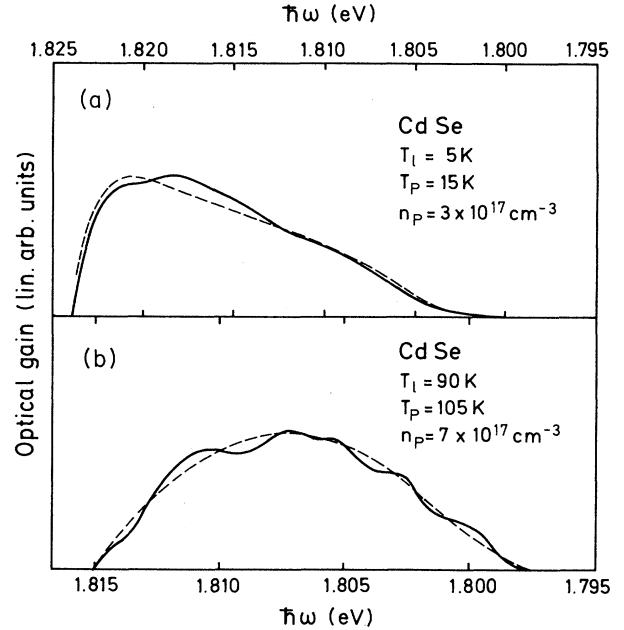


FIG. 4. Measured spectra of optical gain in CdSe under high excitation (solid lines). (a) $T_l = 5 \text{ K}$; (b) $T_l = 90 \text{ K}$. The dashed lines show the calculations according to the many-particle theory for the EHP (Ref. 10) with an assumed n_p of 3×10^{17} and $7 \times 10^{17} \text{ cm}^{-3}$ and a T_p of 15 and 105 K, respectively.

difference between T_l and T_p is rather small due to the strong coupling to the phonon system in these more ionic bound materials [fractional ionic character $\simeq 0.7$ (Ref. 11)]. In more covalent bound materials, e.g., GaAs [fractional ionic character $\simeq 0.3$ (Ref. 11)], where the coupling is weaker, T_p exceeds T_l by more than 100 K in this temperature region and under comparable excitation conditions.¹²

Under constant excitation conditions the shape of the gain spectra changes with increasing temperature, as shown in Fig. 4(b) for $T_p = 105 \text{ K}$. The variation of the quasi-Fermi functions and of the excitonic enhancement with temperature lead to the smoother high-energy side of the spectrum.

The integrated gain, i.e., the area under the gain spectrum decreases with increasing T_p in accordance with the results for CdS presented in Ref. 2. From these experimental data the dependence of n_p on the temperature can be deduced from the comparison with the calculations using the many-particle theory of the EHP mentioned above. Figure 4 already indicates that n_p increases with T_p under constant excitation conditions. This is further elaborated in the following: since the filling of conduction and valence bands in the plasma state with electrons and holes, respectively, is described by the corresponding quasi-Fermi functions, the width of the gain spectra is given by the sum of the quasi-Fermi energies of electrons and holes, $\sum \varepsilon_f^{e,h}$. This value is calculated in dependence of the temperature for CdS and CdSe for different plasma densities, assuming a negligible drift velocity of the EHP (Ref. 2) in Figs. 5(a) and 5(b). In the case of CdS, n_p at

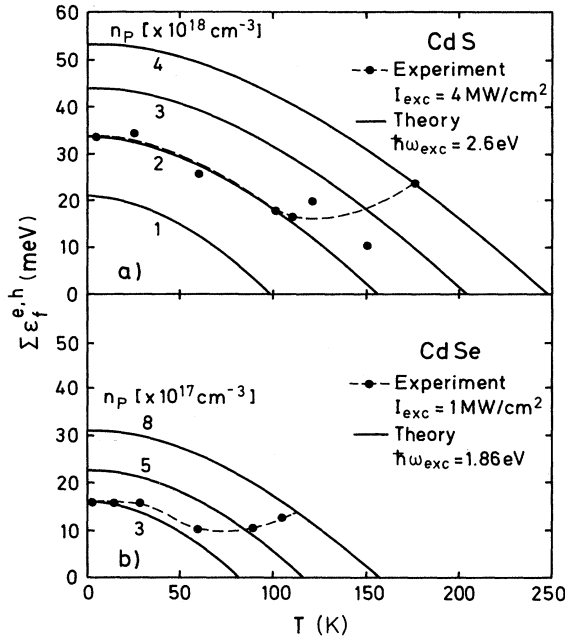


FIG. 5. The sum of the quasi-Fermi energies of electrons and holes as a function of the temperature for different plasma densities. Solid lines, theory; dashed lines, experiments under constant excitation conditions (a) CdS; (b) CdSe.

helium temperature amounts to $2 \times 10^{18} \text{ cm}^{-3}$. Assuming a constant n_p , one would expect a continuously decreasing $\sum \varepsilon_f^{e,h}$ down to zero at around 160 K. That corresponds to a degenerate plasma up to this temperature and a nondegenerate situation for higher temperatures, described by Boltzmann statistics. In fact, the experimental results [dotted line in Fig. 5(a)] reveal a constant n_p only up to 100 K and a linear increase above, as shown in Fig. 6, where n_p is plotted as a function of the temperature for CdS (triangles) and CdSe (circles). At 175 K, n_p has reached CdS with $4 \times 10^{18} \text{ cm}^{-3}$ twice the value at low temperatures.

We observed the same behavior in CdSe, shown in Fig.

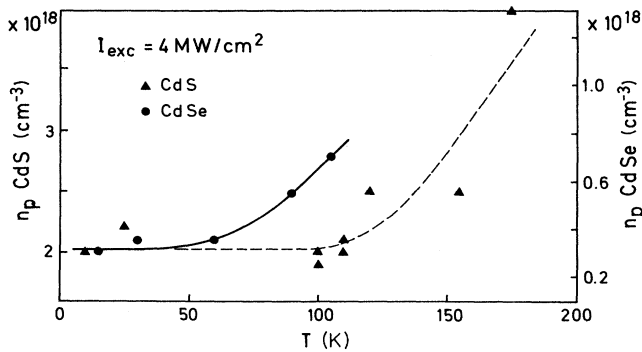


FIG. 6. The density of the plasma n_p in CdS (triangles, left ordinate) and CdSe (circles, right ordinate) under high excitation as a function of the temperature as obtained from the comparison between experiment and many-particle theory.

5(b). For the highest excitation intensities with $n_p = 8 \times 10^{17} \text{ cm}^{-3}$, $\sum \varepsilon_f^{e,h}$ goes below zero also at 160 K. The smaller n_p obtained in the recent experiments compared to Ref. 2 leads to a deviation from the constant value of n_p already at around 70 K and a doubling at 100 K, as can be seen in Fig. 6. Consequently, n_p has been increased by a factor 1.5 with respect to low temperatures in CdS as well as in CdSe at those temperatures, where the transition to a nondegenerate plasma is expected from the calculated T_p dependence of the quasi-Fermi functions. These findings are supported by the increase of the change of the refractive index under excitation with increasing temperature, as it has been shown in Ref. 2.

There are two reasons for this behavior. First, due to the decrease of $\sum \varepsilon_f^{e,h}$ with increasing temperature (Fig. 5) a higher n_p is necessary to reach the situation of a degenerate EHP, according to the modified effective density of state. This results in a decreasing stimulated emission and a decreasing gain with increasing temperature, as observed in the experiments.² Since this recombination mechanism is reduced, the lifetime of the EHP τ_p increases. This will be shown in the next section in discussion of the time-resolved measurements. Second, the drift length of the plasma l_d decreases continuously with increasing temperature, as will be shown in Sec. V.

As a consequence of the temperature behavior of τ_p and l_d , n_p can reach higher values. The corresponding increase of the red shift of the absorption edge cannot be observed due to an exponential absorption tail, which is valid for CdS for temperatures above 90 K.¹³ This so-called Urbach-Martienssen tail determines the absorption edge at high temperatures. The bleaching of this tail leads to a compensation of the red shift and even to an effective blue shift of the absorption edge under excitation for temperatures above 160 K, respectively. As a consequence, apart from the changes of the refractive index, the characteristic features connected with the formation of an electron-hole plasma in CdS and CdSe, namely the gain and red shift of the edge, disappear from the transmission spectra for temperatures higher than 180 K.

B. Time-resolved measurements

Similar to the time-resolved luminescence measurements, we worked here with a multitrack recording system. The gain spectra are recorded in eight temporal consecutive periods (tracks) with temporal width varying between 200 ps and 1 ns. From the evaluation of these spectra we get information about the temporal evolution of the plasma density (Fig. 7) and the change of the refractive index (Fig. 8) for different temperatures. The solid lines present the temporal shape of the exciting laser NDL (narrow-band dye laser), which serves as a source with varying excitation intensity up to an I_{exc} of 4 MW cm^{-2} .

From Fig. 7 we find the following results for the plasma density n_p . At low temperatures (triangles), n_p follows instantaneously the pulse shape of the NDL apart from small deviations at the leading and trailing edges of the pulse. The maximum values of n_p are, of course,

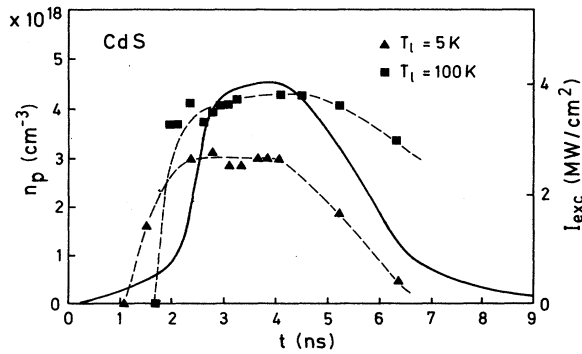


FIG. 7. The temporal behavior of the density of the EHP in CdS at a lattice temperature T_l of 5 K (triangles) and 100 K (squares). The solid line represents the temporal shape of the exciting laser (I_{exc}).

higher than in the time-integrated measurements. At the leading edge of the pulse, n_p starts to saturate at $I_{exc} \simeq 2 \text{ MW cm}^{-2}$, which is in agreement with earlier experiments.¹ In the first spectra taken after the maximum of the exciting pulse NDL_{\max} , n_p has already decreased by about 35%. the same is true for the temporal behavior of the integral optical gain and the chemical potential of the EHP, not shown here. That means that we get no delay between exciting pulse and reaction of the system larger than 200 ps, which is our shortest time interval. This is in accordance with a lifetime τ_p of the EHP of 200 ps, which was also reported earlier by other authors.^{2,14}

In contrast, the onset of $n_p(t)$ at 100 K (squares) shows a delay with respect to $I_{exc}(t)$, and the maximum is reached at later times. Moreover, the decrease of n_p after NDL_{\max} is delayed by $\simeq 400$ ps; 1 ns after NDL_{\max} , n_p has decreased only about 5%. n_p reaches higher values at 100 K than at 5 K, in accordance with the results presented in the time-integrated measurements. The same temporal behavior can be observed in the change of the refractive index Δn at 140 K (squares in Fig. 8). Here

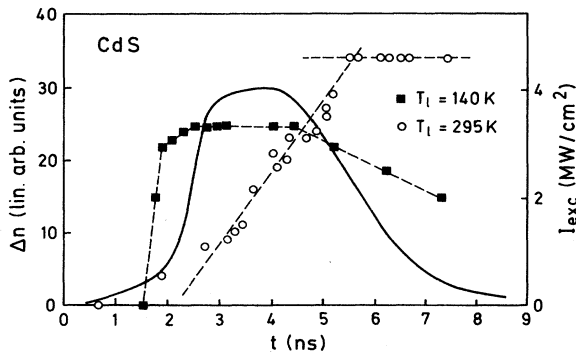


FIG. 8. The temporal behavior of the change of the refractive index as deduced from the shift of the Fabry-Perot modes in arbitrary units at 140 K (squares) and room temperature (open circles). The solid line presents the temporal shape of the exciting laser (I_{exc}).

the absolute shift of the Fabry-Perot modes of the plate-like crystal is taken to show the temporal evolution of Δn as already presented in Ref. 2. We do not show $\Delta n(t)$ at 5 K, since this dependence evolves like $n_p(t)$ with time constants below our temporal resolution. We obtain the same overall retardation in the reaction of the system as we have seen in Fig. 7 at 100 K. We explain this situation with an increase of τ_p to values around 400 ps due to the decrease of the stimulated emission, which leads in turn to the higher values of n_p (see also Sec. III).

This development leads at room temperature to the situation also sketched in Fig. 8 by open circles. The temporal evolution of Δn is strongly retarded and reaches its maximum more than 1 ns after NDL_{\max} . In the temporal range under investigation, a decrease could not even be observed. The values of Δn are again larger at these temperatures in accordance with Ref. 2 and the results of the previous sections. These findings suggest values of τ_p around 1 ns for room temperature.

V. THE EXPANSION OF THE EHP

The gradient of the density and of the chemical potential of the EHP, which appears under surface excitation, leads to a drift into the crystal. We have determined the drift length l_d at 5 K in earlier experiments² to 5 and 12 μm in CdS and CdSe, respectively. The resulting drift velocities for electrons and holes are somewhat larger than a simple diffusion model would suggest. On the other hand, they are smaller than the corresponding Fermi velocities and are thus negligible in connection with the interpretation of the gain spectra. Nevertheless, the drift reduces n_p by a certain amount.

In Fig. 9, new results for l_d are plotted as a function of the temperature on a logarithmic scale, obtained with different experimental techniques as described in Sec. II. Solid circles reflect the investigation of the gain as a function of the crystal thickness, whereas crosses and triangles are deduced from the disappearance of the $A\Gamma_5^T$ - and $B\Gamma_5^T$ -exciton resonances, respectively, from the reflection

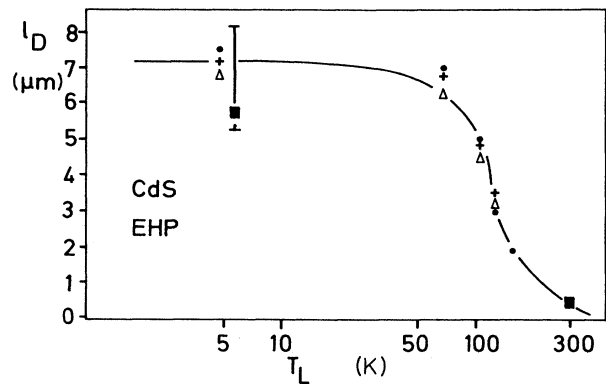


FIG. 9. The drift length l_d of the EHP in CdS as a function of the temperature achieved by investigating the spectrally integrated EHP gain (solid circles), reflection structures of the $A\Gamma_5$ (crosses) and $B\Gamma_5$ (triangles) excitons on the unexcited surface, laser-induced gratings (solid squares) from Refs. 15 and 16.

spectra of the unexcited surface. In addition, results from measurements using laser-induced gratings^{15,16} are shown for comparison (solid squares), which are in good agreement with our values.

The continuous decrease of l_d with increasing temperature can be explained by several mechanisms: first, the influence of scattering with phonons will increase; second, due to the higher n_p the scattering between electrons and holes will also increase. In addition, l_d decreases at temperatures about 150 K, which corresponds to the temperature of the transition from a degenerate to a nondegenerate plasma in CdS, assuming a n_p of $2 \times 10^{18} \text{ cm}^{-3}$ [see Fig. 5(a) in Sec. IV A]. In a degenerate plasma only those particles can participate in scattering processes with small or zero energy transfer, which are situated around the quasi-Fermi energy. Thus, the transition to the nondegenerate state, where all particles are able to scatter with small energy transfer, is also connected with an increase of the scattering probability.

Beside this, the behavior of l_d leads, together with the increase of τ_p presented in the preceding section, to a significant decrease of the drift velocity v_d . At 100 K, v_d has a value of $1 \times 10^6 \text{ cm s}^{-1}$. Taking into account the Fermi velocity to be more or less constant, at least one of the electrons, the neglect of v_d described above is also justified at high temperatures.

VI. UNIVERSALITY OF BAND-GAP RENORMALIZATION

In this section we compare our measured results with theory discussed in literature. In Ref. 17, a universal formula was presented, describing the sum of exchange and correlation energies in an electron-hole liquid in units of the excitonic Rydberg energy. It contains, beside some constants, only the dimensionless parameter r_s given by $r_s = [3/(4\pi \times a_{\text{ex}}^3 \times n)]^{1/3}$, with a_{ex} as the excitonic Bohr radius and n as the density of the excited system. Thus, the properties of the crystal under excitation, e.g., the shrinkage of the band gap ΔE_g as a consequence of exchange and correlation effects turn out to be independent of band characteristics of a specific material. In Fig. 10(a) the dotted line presents ΔE_g in units of the excitonic Rydberg Ry as a function of r_s according to Ref. 17. We calculated r_s by using the density of an EHP as evaluated from our measurements with the help of the many-particle theory in Sec. IV, and an a_{ex} , e.g., for CdS of 2.8 nm.

In a recent work,¹⁸ Zimmermann proposed another expression for ΔE_g as a function of the density and of the temperature in connection with the description of the Mott transition: $\Delta E_g(n, T) = (-3.24r_s^{-3/4})(1 + 0.0478r_s^3J^2)^{1/4}$, where $J = k_B T R_y^{-1}$. Expressing r_s in terms of the plasma density, this equation leads to the known $n^{1/4}$ dependence of exchange and correlation energies in an EHP. This relation is plotted in Fig. 10(a) for three different temperatures ($T = 30, 150$ and 300 K) as solid lines. For low densities (i.e., large r_s) the results from Ref. 17 correspond to Zimmermann's approach for low temperatures. For high densities the

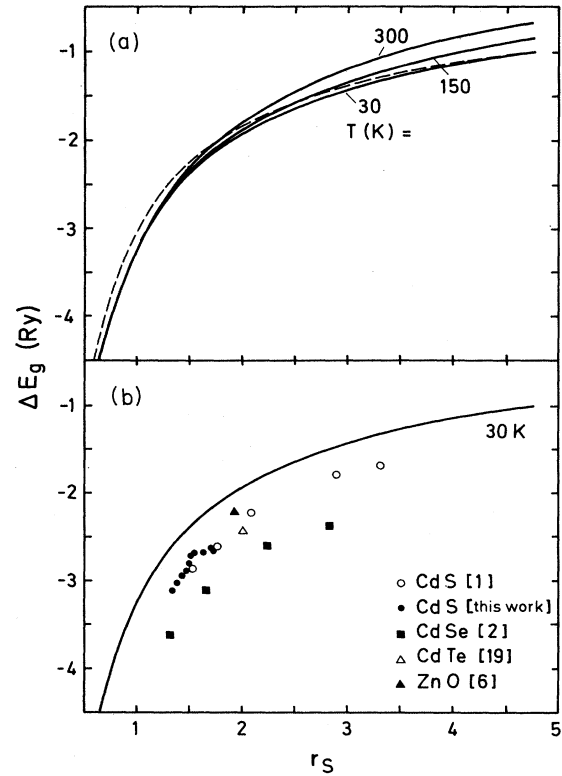


FIG. 10. (a) The shrinkage of the band gap in units of the excitonic Rydberg as a function of r_s : dashed line, Vashishta *et al.* (Ref. 17); solid lines, Zimmermann (Ref. 18) for $T = 30, 150$, and 300 K . (b) Comparison between theory from Ref. 18 for $T = 30 \text{ K}$ and experimental data: open circles, CdS from Ref. 1; solid circles, CdS from Sec. IV; squares, CdSe from Ref. 2, open triangle, CdTe from Refs. 2 and 19, solid triangle, ZnO from Ref. 6. For more information, see text.

latter one gets independent of the temperature.

In Fig. 10(b), ΔE_g ($T = 30 \text{ K}$) according to Zimmermann is compared with results from several measurements on II-VI materials: CdS for low temperatures from Ref. 1 (open circles) and for $5 \text{ K} \leq T \leq 150 \text{ K}$ from the results presented in Sec. IV (solid circles), CdSe for low temperatures from Ref. 2 (squares, $a_{\text{ex}} = 4.72 \text{ nm}$, $R_y = 17.5 \text{ meV}$), CdTe from Ref. 19 (open triangle, $a_{\text{ex}} = 6.7 \text{ nm}$, $R_y = 12 \text{ meV}$), and ZnO from Ref. 6 (solid triangle, $a_{\text{ex}} = 1.8 \text{ nm}$, $R_y = 60.8 \text{ meV}$).

The measured overall behavior of ΔE_g as a function of r_s can be described with the theory as it can be seen especially for CdS and CdSe. Nevertheless, the absolute values of ΔE_g deduced from experiment are too large, and the difference between experimental data and theory from Ref. 17 is even larger. These discrepancies seem to be a result of the ionic character of the II-VI compounds, because results for Ge, Si, or GaAs can be described quite well in this theoretical frame.^{17,18} In the ionic bound semiconductors we deal with the following situation: since the radii of exciton and polaron have comparable values, the band renormalization due to exciton-phonon interaction which leads to the so-called polaron gap is

rather pronounced.⁴ As a result, the Rydberg energy of the 1s exciton is larger than the binding energy seen in the experiment. A rescaling of Ry to larger values would in turn bring the experimental data closer to the calculated curve. The modified masses would also change the excitonic Bohr radii, and thus r_s .

VII. COMPARISON WITH THE MIXED CRYSTALS $\text{CdS}_{1-x}\text{Se}_x$

Finally, we want to compare the pure crystals CdS and CdSe with the alloy system $\text{CdS}_{1-x}\text{Se}_x$. In these mixed crystals, localization effects due to compositional disorder play a dominating role at temperatures below 60 K.²⁰⁻²⁴ The fluctuating composition leads to fluctuations in the crystal potential, where optically created excitons get localized within 50 ps after excitation.²⁴ This process evolves eventually via the localization of the hole in the valence band and the Coulomb interaction between electron and hole. The fluctuations lead to an exponential tail in the density of states, which can be observed in the time-integrated luminescence spectra at low temperatures as a broad band without specific features. The lifetimes of the localized excitons are three times longer than those of free excitons and they depend on the spectral position. This can be observed in the temporal behavior of the rise and decay time in time-resolved measurements.^{22,24-27} In two-beam experiments we obtain at low temperatures a bleaching of these localized states resulting in a blue shift of the absorption edge under excitation. Besides,

many-particle effects, which lead in the pure constituents to an EHP, can be neglected due to the decreased mobility of the localized excitons.^{23,25-27} Characteristic features of the EHP-like gain and red shift of the absorption edge under excitation can only be observed at temperatures above 60 K, where a delocalization due to a thermal reexcitation of the excitons out of the localized states occurs. This behavior can also be seen in the time-integrated and time-resolved luminescence measurements. The optical properties of $\text{CdS}_{1-x}\text{Se}_x$ above 60 K are essentially the same as in the pure constituents and dominated by the formation of an EHP under high excitation. Experiments with laser-induced gratings showed reduced diffusion coefficients indicating a reduced but nonzero mobility of the excitons in the localized states and increased phase relaxation times. For details concerning these experiments the reader is referred to the literature, e.g., Refs. 22-27.

ACKNOWLEDGMENTS

This work is part of a project of the Sonderforschungsbereich 185 "Nichtlineare Dynamik" supported by the Deutsche Forschungsgemeinschaft. For one of the authors (M.S.) the European Community has provided a travel grant in the frame of the PROCOPE project. The high-quality CdS and CdSe crystals have been grown at the crystals laboratories at the Universities of Strasbourg and Karlsruhe.

*Permanent address: Institute de Physique et Chimie des Matériaux de Strasbourg, Groupe d'Optique Nonlineaire et d'Optoelectronique, 5 rue de l'Université, F-67084 Strasbourg CEDEX, France.

¹K. Bohnert, M. Anselment, G. Kobbe, C. Klingshirn, H. Haug, S. W. Koch, S. Schmitt-Rink, and F. F. Abraham, *Z. Phys. B* **42**, 1 (1981).

²M. Majumder, H.-E. Swoboda, K. Kempf, and C. Klingshirn, *Phys. Rev. B* **32**, 2407 (1985); H.-E. Swoboda, F. A. Majumder, V. G. Lysenko, C. Klingshirn, and L. Banyai, *Z. Phys. B* **70**, 341 (1988).

³*Semiconductors: Physics of II-VI and I-VII Compounds, Semimagnetic Semiconductors*, Vol. 17b of *Landolt-Börnstein, New Series*, edited by O. Madelung, M. Schulz, and H. Weiss (Springer-Berlin, Heidelberg, 1982), Group III.

⁴C. Klingshirn and H. Haug, *Phys. Rep.* **70**, 315 (1981).

⁵C. Dörnfeld and J. M. Hvam, *J. Phys. C* **2**, 205 (1988); C. Dörnfeld and J. M. Hvam, *IEEE J. Quantum Electron.* (to be published).

⁶K. Bohnert, G. Schmieder, and C. Klingshirn, *Phys. Status Solidi B* **98**, 175 (1980); C. Klingshirn, *Solid State Commun.* **13**, 297 (1973).

⁷E. F. Gross, S. A. Permogorov, and B. S. Razbirin, *Usp. Fiz. Nauk* **103**, 431 (1971) [*Sov. Phys.—Usp.* **14**, 104 (1971)]; S. A. Permogorov, in *Excitons*, edited by E. I. Rashba and M. D. Sturge (North-Holland, Amsterdam, 1982).

⁸V. A. Abramov, S. A. Permogorov, B. S. Razbirin, and A. I. Ekimov, *Phys. Status Solidi B* **42**, 627 (1970).

⁹C. Klingshirn, *Phys. Status Solidi B* **71**, 547 (1975).

¹⁰S. Schmitt-Rink, J. P. Löwenau, H. Haug, K. Bohnert, A. Kreissl, K. Kempf, and C. Klingshirn, *Physica* **117-118B**, 339 (1983).

¹¹C. Kittel, *Introduction to Solid State Physics*, 4th ed. (Wiley, New York, 1971), p. 124.

¹²C. Klingshirn, Ch. Weber, D. S. Chemla, D. A. B. Miller, J. E. Cunningham, C. Ell, and H. Haug, *Proceedings of the Workshop on Optical Switching in Low-Dimensional Systems*, Marbella, Spain, 1988 (to be published).

¹³D. Dutton, *Phys. Rev.* **112**, 785 (1958).

¹⁴H. Saito and E. O. Göbel, *Phys. Rev. B* **31**, 2360 (1985).

¹⁵C. Weber, U. Becker, R. Renner, and C. Klingshirn, *Appl. Phys. B* **45**, 113 (1988).

¹⁶C. Weber, U. Becker, R. Renner, and C. Klingshirn, *Z. Phys. B* **72**, 379 (1988).

¹⁷P. Vashishta and R. K. Kalia, *Phys. Rev. B* **25**, 6492 (1982).

¹⁸R. Zimmermann, *Phys. Status Solidi B* **146**, 371 (1988).

¹⁹H. Schweizer and E. Zielinski, *J. Lumin.* **31 and 32**, 503 (1984).

²⁰S. A. Permogorov, A. Reznitsky, P. Flögel, S. Verbin, G. O. Müller, and M. Nikiforova, *Phys. Status Solidi B* **113**, 589 (1982).

²¹E. Cohen and M. D. Sturge, *Phys. Rev. B* **25**, 3828 (1982).

²²H.-E. Swoboda, F. A. Majumder, C. Klingshirn, S. Shevel, R. Fischer, E. O. Göbel, G. Noll, P. Thomas, S. Permogorov, and A. Reznitsky, *J. Lumin.* **38**, 79 (1987).

²³F. A. Majumder, S. Shevel, V. G. Lyssenko, H.-E. Swoboda, and C. Klingshirn, *Z. Phys. B* **66**, 409 (1987).

²⁴S. Shevel, R. Fischer, E. O. Göbel, G. Noll, P. Thomas, and C.

- Klingshirn, J. Lumin. **37**, 45 (1987).
- ²⁵F. A. Majumder, H.-E. Swoboda, and C. Klingshirn, *Proceedings of the International Conference on Luminescence Science and Technology, Chicago, 1988* [J. Electrochem. Soc. (1989)].
- ²⁶H.-E. Swoboda, F. A. Majumder, R. Renner, C. Weber, M. Sence, Lu Jie, G. Noll, E. O. Göbel, J. Vaitkus, and C. Klingshirn, Phys. Status Solidi B **150**, 749 (1988).
- ²⁷H.-E. Swoboda, F. A. Majumder, C. Weber, R. Renner, C. Klingshirn, G. Noll, E. O. Göbel, S. A. Permogorov, and A. Reznitsky, *Proceedings of the 19th International Conference on the Physics of Semiconductors, Warsaw, Poland, 1988* (Scientific and Technical Publishers, Warsaw, 1989).